Arts, Karsten; Vandalon, Vincent; Puurunen, Riikka L.; Utriainen, Mikko; Gao, Feng; Erwin Kessels, Wilhelmus M.M.; Knoops, Harm C.M.

Sticking probabilities of H_2O and $Al(CH_3)_3$ during atomic layer deposition of Al_2O_3 extracted from their impact on film conformality

Published in:
Journal of Vacuum Science and Technology A: Vacuum, Surfaces and Films

DOI:
10.1116/1.5093620

Published: 24/04/2019

Document Version
Publisher's PDF, also known as Version of record

Sticking probabilities of H_2O and $Al(CH_3)_3$ during atomic layer deposition of Al_2O_3 extracted from their impact on film conformality

Karsten Arts, Vincent Vandalon, Riikka L. Puurunen, Mikko Utriainen, Feng Gao, Wilhelmus M. M. (Erwin) Kessels, and Harm C. M. Knoops

Citation: Journal of Vacuum Science & Technology A **37**, 030908 (2019); doi: 10.1116/1.5093620
View online: https://doi.org/10.1116/1.5093620
View Table of Contents: https://avs.scitation.org/toc/jva/37/3
Published by the American Vacuum Society

Sticking probabilities of H_2O and $Al(CH_3)_3$ during atomic layer deposition of Al_2O_3 extracted from their impact on film conformality

Karsten Arts,[1,a)] Vincent Vandalon,[1] Riikka L. Puurunen,[2,3] Mikko Utriainen,[3] Feng Gao,[3] Wilhelmus M. M. (Erwin) Kessels,[1] and Harm C. M. Knoops[1,4,b)]
[1]*Department of Applied Physics, Eindhoven University of Technology, P.O. Box 513, 5600 MB Eindhoven, The Netherlands*
[2]*Aalto University School of Chemical Engineering, Aalto University, Kemistintie 1, Espoo, P.O. Box 16100, FI-00076 Aalto, Finland*
[3]*VTT Technical Research Centre of Finland, Tietotie 3, 02044 Espoo, Finland*
[4]*Oxford Instruments Plasma Technology, North End, Bristol BS49 4AP, United Kingdom*

(Received 22 February 2019; accepted 8 April 2019; published 24 April 2019)

The conformality of a film grown by atomic layer deposition (ALD) is strongly affected by the reactivities of the precursor and coreactant, which can be expressed in terms of their sticking probabilities toward the surface. We show that the leading front of the thickness profile in high-aspect-ratio structures gives direct information on the sticking probabilities of the reactants under most conditions. The slope of the front has been used to determine the sticking probabilities of $Al(CH_3)_3$ and H_2O during ALD of Al_2O_3. The determined values are $(0.5–2)\times10^{-3}$ for $Al(CH_3)_3$ and $(0.8–2)\times10^{-4}$ for H_2O at a set-point temperature of 275 °C, corresponding to an estimated substrate temperature of ~220 °C. Additionally, the thickness profiles reveal soft-saturation behavior during the H_2O step, most dominantly at reduced temperatures, which can limit the conformality of Al_2O_3 grown by ALD. This work thus provides insights regarding quantitative information on sticking probabilities and conformality during ALD, which is valuable for gaining a deeper understanding of ALD kinetics. *Published by the AVS.* https://doi.org/10.1116/1.5093620

I. INTRODUCTION

Atomic layer deposition (ALD), which makes use of self-limiting precursor and coreactant steps,[1–3] has become an enabling technique for the preparation of ultrathin films on the increasingly demanding 3D structures used in applications such as memory cells and transistors.[4,5] The self-limiting nature of ALD ideally yields a constant thickness of a film deposited over a high-aspect-ratio (AR) substrate. In reality, a nonideal thickness profile can be obtained, which is strongly dependent on the dose and reactivity of the precursor and coreactant.[6–8] Moreover, in cases where the dose has to be extended to reach conformal coating, the required extension can depend strongly on the reactivity of the dosed reactant.[9,10] The effect of dose and reactivity on conformality is qualitatively described in the literature through theoretical and experimental studies,[11] where the reactivities of the reactants are typically expressed in terms of their sticking probabilities toward the surface. Only a few studies focus on acquiring quantitative information on sticking probabilities,[12–15] while such quantitative information is essential for the understanding and modeling of different ALD processes.

This work provides a method to directly extract initial sticking probabilities from thickness profiles acquired in high AR structures. Here, we note that the slope of the leading front of the thickness profile in such structures is determined by the reactivity of the reactant that penetrates the structure the least deep. Using this relation, the sticking probabilities of H_2O and $Al(CH_3)_3$ trimethylaluminum (TMA) during ALD of Al_2O_3 have been determined, where the sticking probability of H_2O is observed to increase with temperature. Moreover, we observe that the Al_2O_3 thickness profiles indicate a non-Langmuir saturation component during the H_2O step. This "soft-saturation," which is most prominent at reduced temperatures, can be an important factor limiting the conformality of Al_2O_3 deposited by ALD.

II. EXPERIMENT AND MODELING

A. High-aspect-ratio structures for conformality analysis

As recently reviewed by Cremers *et al.*,[11] several high AR structures have been used in the literature to assess the conformality of ALD processes, such as vertical trenches,[16–19] pillars,[20–23] and porous materials.[24,25] Alternatively, lateral structures can be employed[6,7,26,27] which allow for top-view diagnostics to easily and accurately quantify the conformality and properties of the deposited film. The microscopic lateral-high-aspect-ratio (LHAR) trenches developed by Puurunen and co-workers,[7,14,28,29] named as PillarHall® technology, have been adopted in this work. In the used third generation LHAR structures (LHAR3), a polysilicon membrane, supported by a network of Si pillars, is suspended above a c-Si substrate with a nominal gap height of 500 nm. Elongated openings in the membrane allow for diffusion of the ALD reactants into the lateral trench up to a depth of 5 mm, corresponding to an AR of 10 000. In such an extremely high AR feature, the reactants typically do not reach the end of the feature during deposition, resulting in a diffusion-limited thickness profile.[30] Figure 1(c) gives a schematic cross-

Note: This paper is part of the 2019 special collection on Atomic Layer Deposition (ALD).
a)Electronic mail: k.arts@tue.nl
b)Electronic mail: h.c.m.knoops@tue.nl

sectional side view of an LHAR3 structure, also showing a typical profile of a film grown by ALD. After deposition, the membrane can be removed using adhesive tape, and the Al_2O_3 thickness profile can be resolved using a technique such as reflectometry.

B. Simulating ALD thickness profiles in 1D structures

Comparing experimentally obtained thickness profiles with simulated profiles can provide the initial sticking probability s_0 of the used ALD reactant, as shown for instance by Rose and Bartha[12] and Ylilammi *et al.*[14] Here, s_0 indicates the sticking probability toward the initial surface on which all reaction sites are still available. In several models, e.g., ballistic,[8,31–35] continuum,[14,36–38] and Monte Carlo,[9,10,12,27,30,39–42] it is observed that s_0 governs the slope of the leading front of the thickness profile. In this work, the relation between the slope of the profile front and the initial sticking probability has been quantified using the continuum model reported by Yanguas-Gil and Elam[36] to directly determine sticking probabilities from ALD thickness profiles without further modeling.

The adopted continuum model can be summarized as follows.[36] For a 1D system with a constant diffusion coefficient D ($m^2\,s^{-1}$), the evolution of gas-phase reactant density $n(z,t)$ (m^{-3}) and surface coverage $\theta(z,t)$ is generically described by the following dimensionless reaction-diffusion equations:[36]

$$\frac{\partial\tilde{n}}{\partial\tau}-\frac{\partial^2\tilde{n}}{\partial\xi^2}=-\alpha(1-\theta)\tilde{n}, \tag{1}$$

$$\frac{d\theta}{d\tau}=\alpha\gamma(1-\theta)\tilde{n}. \tag{2}$$

Here, $\tilde{n}\equiv n/n_0$ is the reactant density normalized by the density n_0 (m^{-3}) at the entrance of the high AR structure at $z=0$. The penetration depth z (m) is normalized by the total structure length L (m) such that $\xi\equiv z/L$ and the dimensionless time is given by $\tau\equiv tD/L^2$. In these equations, the surface coverage θ is defined as the reacted fraction of available reaction sites, in such a way that $\theta=1$ in saturation.[6,36] The surface chemistry is simplified by the adopted irreversible Langmuir model, which assumes that the reaction probability is directly proportional to the unreacted fraction of reaction sites $(1-\theta)$.[6,36,43] As described by Eqs. (1) and (2), ALD in a 1D structure is governed by the dimensionless parameters $\alpha\equiv(1/4)L^2(S/V)(v_{th}/D)s_0$ and $\gamma\equiv(Vn_0A_0/S)$, where S/V is the surface to volume ratio of the structure, v_{th} is the mean thermal velocity ($m\,s^{-1}$), and A_0 is the average area (m^2) of an adsorption site, which can be calculated from the growth per cycle.[14,36] The parameter α describes the ratio between the reaction rate and diffusion rate, while γ describes the number of reactant molecules simultaneously present in the structure per adsorption site. For a typical feature size (e.g., a trench with a cavity height h of 500 nm) and process pressure (e.g., 100 mTorr), θ changes much slower than $\tilde{n}$ as $\gamma\ll1$.[36] In these cases, the evolution of the coverage profile $\theta(\xi)$ only depends on α.[36] Moreover, Knudsen diffusion can be assumed as the mean free path $\lambda_{mfp}\sim 0.1\text{mm}\gg h$.[11] This gives $\alpha=(3/4)(L/h)^2s_0$ for a trench with width $w\gg h$ (m), where $(S/V)=(2/h)$ and $D=(2/3)v_{th}h$ such that v_{th} cancels out.[14] Under these conditions, the coverage profile is solely determined by the reactant dose and initial sticking probability.

C. Relation between profile slope and sticking probability

Since the coverage profile is governed by the dose and reactivity of the reactant, it can be used to extract its initial sticking probability. This is illustrated in Fig. 1, which shows general results obtained using the adopted continuum model.[36] Figure 1(a) demonstrates that an increase in dose results in an increase in penetration depth, while the shape of the profile front stays the same. Indeed, we have verified that the slope at the front of the modeled profiles remains constant for an extensive range of doses. This slope is only determined by the initial sticking probability, as shown in Fig. 1(b). For low reactivities, e.g., $s_0=10^{-4}$, it takes longer to saturate the surface. During this longer saturation time, the reactant diffuses deeper into the feature, resulting in a broader diffusion front. For relatively high values of s_0, e.g., 10^{-2}, the surface saturates quickly when the reactant diffuses inward, resulting in a sharp profile front. For the axes in Fig. 1, a trench structure is assumed and the penetration depth is normalized by the cavity height such that $\tilde{z}\equiv z/h$. Under this normalization, the relation between the slope $\partial\theta/\partial\tilde{z}$ at the point of half coverage $\theta=1/2$ and the initial sticking probability s_0 is computed to be

$$\left|\frac{\partial\theta}{\partial\tilde{z}}\right|_{\theta=1/2}\approx\sqrt{s_0/13.9}. \tag{3}$$

As clarified in Fig. 1(d), relation (3) is obtained by determining the slopes of the modeled profiles as a function of s_0 and fitting these data with a square root function. While Eq. (3) generally applies to trench structures, it can be further generalized by using the equivalent aspect ratio (EAR)[11] of the structure of interest instead of $\tilde{z}$. For example, $EAR=(z/2h)=(\tilde{z}/2)$ for a trench, while $EAR=z/r$ for a pore with radius r.[44] Note that relation (3) is in line with coverage profiles obtained by Monte Carlo simulations[11] which affirms its applicability.

III. RESULTS AND DISCUSSION

Equation (3) can thus be used to calculate the initial sticking probability of the dosed reactant using the coverage profile, which is experimentally determined as a normalized thickness profile. Still, note that the thickness profile acquired after ALD is only proportional to this coverage profile when the other reactant is in saturation and has a higher penetration depth. Hence, although often not considered in the literature, the slope of the profile front is determined by the reactivity of the reactant with the lowest penetration depth. In this work, an Al_2O_3 thickness profile is called "TMA-limited" if TMA penetrates less deep into the feature than H_2O. If the penetration

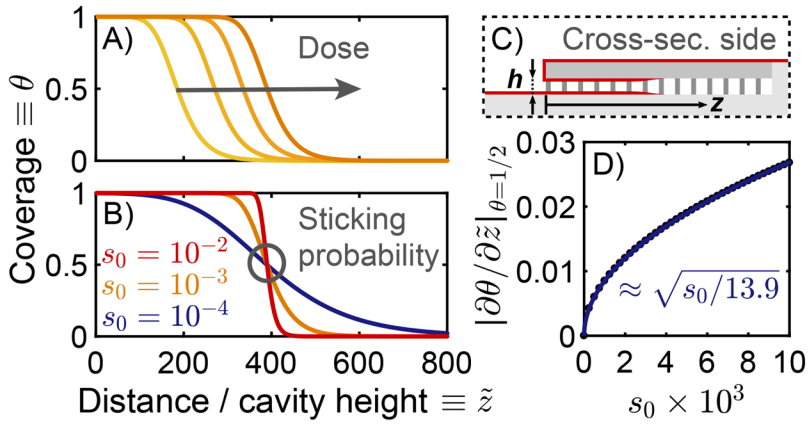

FIG. 1. Modeled (Ref. 36) coverage profiles for a varied precursor dose (a) and initial sticking probability (b). Experimentally, such coverage profiles are acquired as normalized thickness profiles of films deposited in LHAR structures (Refs. 7, 14, 28, and 29) of which a schematic cross-sectional side view is given in panel (c). Panel (d) gives the extracted relation between the slope at the profile front and the value of the initial sticking probability.

depth of TMA is higher than that of H_2O, the profile is called "H_2O-limited."

The difference between TMA-limited and H_2O-limited growth is determined in Fig. 2, which shows normalized thickness profiles of the Al_2O_3 deposited in LHAR3 structures with varied TMA dosing. These profiles are measured using reflectometry by a Filmetrics F40 with XY10 stage and a spot size of 10 μm. For the profile with the highest penetration depth, a high TMA dose was used (~1200 mTorr s TMA dose, ~750 mTorr s water dose, Oxford Instruments OpAL reactor) such that the H_2O step was limiting film penetration. For the central profile, the TMA dose was reduced (~190 mTorr s) to obtain a TMA-limited profile. This profile has a sharper diffusion front than the H_2O-limited profile, indicating that TMA is more reactive than H_2O. A similar high slope was observed by Ylilammi *et al.*[14] (left) who also seem to have used TMA-limited growth conditions (<225 mTorr s TMA dose, <225 mTorr s water dose, Picosun

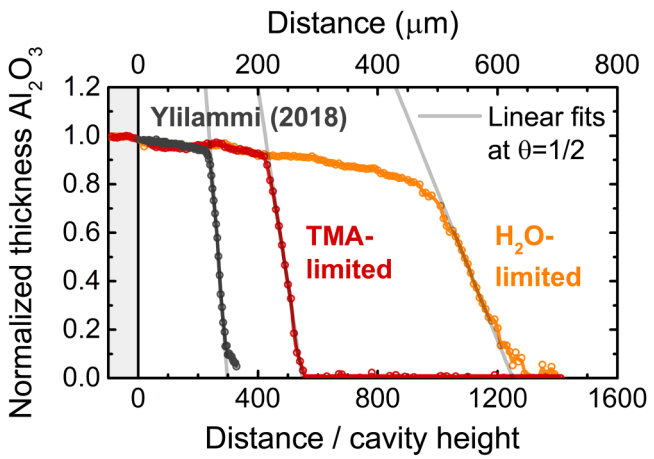

FIG. 2. Normalized thickness profiles of Al_2O_3 deposited in LHAR3 structures with varied TMA dosing, as obtained by Ylilammi *et al.* (left, 300 °C) (Ref. 14) and in this work (T_{set} = 275 °C). When the penetration depth of TMA is lower than that of H_2O (called TMA-limited, middle), the profile has a sharper front than when TMA penetrates deeper than H_2O (called H_2O-limited, right). This can be attributed to the higher sticking probability of TMA compared to H_2O.

R-150 reactor). Note that such knowledge on the reactant doses, e.g., the evolution of pressure in the reactor, can be used to analytically[14,44] estimate the penetration depths of the reactants and determine which reactant is limiting the film conformality. In our case, the estimated penetration depths, i.e., ~220 and ~550 μm for 190 and 1200 mTorr s TMA dose, respectively, and ~500 μm for 750 mTorr s water dose, are indeed in line with our TMA- and H_2O-limited profiles plotted in Fig. 2.

In Fig. 2, the slopes at 50%-thickness-penetration-depth ($PD^{50\%}$)[11,14] have been fitted to calculate the initial sticking probabilities of the limiting reactants using Eq. (3). As shown in Table I, the calculated initial sticking probabilities, $(0.5–2)\times10^{-3}$ for TMA and $(0.8–2)\times10^{-4}$ for H_2O at a set temperature of 275 °C, compare well with the results reported in the literature, e.g., by sum-frequency generation (SFG).[15] Note that several sticking probabilities for the TMA/water process have been reported in the literature[14,15,39,45–49] and that our comparison focuses on recent work. In this work, the lower and upper limits of s_0 are computed assuming <10% variation in reactant dosing and ~10 nm uncertainty in cavity height. A natural variation in reactant dosing can lead to broadening of the profile front and thus a lower value of the calculated sticking probability. This effect can be significant in the case of a profile with a sharp front. Broadening of the front due to the narrowing of the trench during deposition (400 cycles, ~46 nm Al_2O_3) has a virtually negligible effect on the profiles reported in this work. In the case of H_2O, the reactivity depends significantly on the temperature of the substrate.[15,48,49] For the set temperature of T_{set} = 275 °C, the actual substrate temperature is estimated to be ~220 °C, while the 300 °C reported by Vandalon *et al.* was measured directly at the substrate itself.[15] The somewhat lower value of s_{0,H_2O} obtained at T_{set} = 275 °C compared with the result obtained by Vandalon *et al.* at 300 °C seems to be in line with the expected reduction in s_{0,H_2O} at lower temperatures. This temperature-dependence of the reactivity of H_2O has been studied further as shown in Fig. 3.

Figure 3(a) shows thickness profiles of Al_2O_3 deposited at different temperatures, where the penetration depth of TMA is higher than that of H_2O. For these H_2O-limited profiles, a

TABLE I. Comparison of initial sticking probabilities s_0 of TMA and H_2O during ALD of Al_2O_3, determined using thickness profiles obtained in LHAR structures [this work and Ylilammi *et al.* (Ref. 14)] and by SFG (Ref. 15). The values calculated from the slopes of the profile fronts [using Eq. (3)] show good correspondence with the SFG data.

Method	Data	T_{set} (°C)	$s_{0,\,TMA}$	s_{0,H_2O}
LHAR, relation Arts [Eq. (3)]	This work (Fig. 2)	275	$(0.5–2)\times10^{-3}$	$(0.8–2)\times10^{-4}$
LHAR, relation Arts [Eq. (3)]	Ylilammi *et al.* (Ref. 14)	300	$(2–7)\times10^{-3}$	—
LHAR, fit Ylilammi *et al.* (Ref. 14)	Ylilammi *et al.* (Ref. 14)	300	5.72×10^{-3}	—
Sum-frequency generation	Vandalon *et al.* (Ref. 15)	300	$(4\pm1)\times10^{-3}$	$(4\pm1)\times10^{-4}$

temperature-dependent reactivity of H_2O toward the surface after TMA exposure can be inferred from the slope at $PD^{50\%}$, which becomes steeper with temperature. The calculated s_0 values of H_2O are plotted in Fig. 1(b) as a function of the substrate temperature, together with values obtained by Vandalon *et al.* using SFG.[15] Both methods give comparable results, showing that the initial sticking probability of H_2O increases by a factor of ~10 when going from 150 to 300 °C. Note that SFG measures s_0 by monitoring the surface chemistry, while our LHAR method is based on the resulting film thickness. The correspondence between these very different approaches affirms that our method is a powerful and straightforward way to estimate sticking probabilities during ALD.

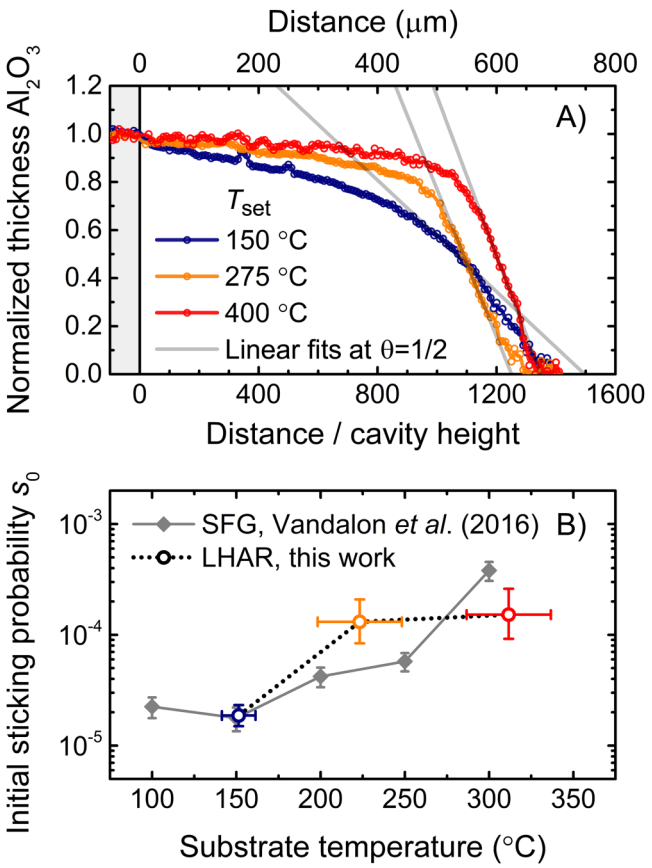

FIG. 3. Panel (a) shows thickness profiles of Al_2O_3 deposited at different set temperatures, where the penetration depth of TMA is higher than that of H_2O. For these H_2O-limited profiles, the temperature-dependent reactivity of H_2O is reflected in the increasing slope at the profile front. The initial sticking probabilities of H_2O corresponding to these slopes are plotted against the substrate temperature in panel (b). Due to limited thermal contact, the substrate temperatures of ~150, ~220, and ~310 °C are typically lower than the set table temperatures of 150, 275, and 400 °C and are therefore estimated based on calibration. The determined values of s_0 (dotted line) show a similar trend as those obtained by Vandalon *et al.* using SFG (solid line) (Ref. 15).

It should be noted that nonideal ALD saturation behavior is observed as well in Figs. 2 and 3. The experimentally obtained thickness profiles, namely, show a decrease in thickness in the region where a saturated thickness is expected based on the Langmuir model [see, e.g., Fig. 1(a)]. Based on Fig. 2, this decrease is largely independent of the TMA dose, which suggests that it is caused by soft-saturation during the H_2O step.[2] Moreover, Fig. 3 reveals that the initial decrease in thickness is most dominant at reduced temperatures, i.e., for 150 °C. These results indicate that soft-saturation during the H_2O step can limit the conformality of ALD-grown Al_2O_3 and that a high deposition temperature or an overdose of H_2O may be required to achieve optimal conformality. This impact of soft-saturation on film conformality is typically not experimentally observed when using a structure with a relatively low AR, where the reactant dose is approximately constant throughout the feature. Moreover, while the profile front gives direct information on s_0, this study exemplifies how analysis of the full thickness profile can provide additional information on the kinetics of the ALD process. Such information on ALD kinetics is not only relevant for film conformality, but also, e.g., wafer-scale uniformity and throughput considerations in terms of time needed for an ALD process per wafer.

IV. CONCLUSIONS

In conclusion, we have established a method to directly determine sticking probabilities during ALD from thickness profiles obtained in high-aspect-ratio structures. While in this work, lateral-high-aspect-ratio trenches were used, the method can be applied to other 3D features as well. As a demonstration, the initial sticking probabilities s_0 of $Al(CH_3)_3$ and H_2O during ALD of Al_2O_3 were determined, giving $(0.5–2)\times10^{-3}$ for $Al(CH_3)_3$ and $(0.8–2)\times10^{-4}$ for H_2O at $T_{set}=275$ °C ($T_{sub}\sim220$ °C). The s_0 value of H_2O was shown to be temperature-dependent, decreasing to $(1.5–2.3)\times10^{-5}$ at 150 °C. These values compare well with literature values obtained by other methods. Furthermore, the Al_2O_3 thickness profiles indicated significant soft-saturation behavior during the H_2O step at reduced temperatures, which can be an important factor limiting the conformality of Al_2O_3 grown by ALD

under these conditions. The aforementioned insights aid in obtaining quantitative information on sticking probabilities and conformality during ALD and in gaining a better understanding of ALD kinetics in general.

ACKNOWLEDGMENTS

This work is part of the research program HTSM with Project No. 15352, which is (partly) financed by the Netherlands Organization for Scientific Research (NWO). M. Bouman and Filmetrics are acknowledged for carrying out the reflectometry measurements. V.T.T. acknowledges the financial support for developing the LHAR3 conformality test structure from the Academy of Finland through the Finnish Centre of Excellence on Atomic Layer Deposition and from Business Finland (National Innovation Funding Center of Finland, previously: Tekes) through the PillarHall TUTL project.

[1]T. Suntola, Mater. Sci. Rep. **4**, 261 (1989).
[2]R. L. Puurunen, J. Appl. Phys. **97**, 121301 (2005).
[3]S. M. George, Chem. Rev. **110**, 111 (2010).
[4]C. S. Hwang, *Atomic Layer Deposition for Semiconductors* (Springer, New York, 2012).
[5]H. C. M. Knoops, S. E. Potts, A. A. Bol, and W. M. M. Kessels, *Handbook of Crystal Growth Thin Films and Epitaxy* (Elsevier, New York , 2014), pp. 1101–1134.
[6]J. Dendooven, D. Deduytsche, J. Musschoot, R. L. Vanmeirhaeghe, and C. Detavernier, J. Electrochem. Soc. **156**, P63 (2009).
[7]F. Gao, S. Arpiainen, and R. L. Puurunen, J. Vac. Sci. Technol. A **33**, 010601 (2015).
[8]A. Yanguas-Gil and J. W. Elam, Theor. Chem. Acc. **133**, 1465 (2014).
[9]V. Cremers, F. Geenen, C. Detavernier, and J. Dendooven, J. Vac. Sci. Technol. A **35**, 01B115 (2017).
[10]P. Poodt, A. Mameli, J. Schulpen, W. M. M. (Erwin) Kessels, and F. Roozeboom, J. Vac. Sci. Technol. A **35**, 021502 (2017).
[11]V. Cremers, R. L. Puurunen, and J. Dendooven, Appl. Phys. Rev. **6**, 021302 (2019).
[12]M. Rose and J. W. Bartha, Appl. Surf. Sci. **255**, 6620 (2009).
[13]M. Rose, J. W. Bartha, and I. Endler, Appl. Surf. Sci. **256**, 3778 (2010).
[14]M. Ylilammi, O. M. E. Ylivaara, and R. L. Puurunen, J. Appl. Phys. **123**, 205301 (2018).
[15]V. Vandalon and W. M. M. Kessels, Appl. Phys. Lett. **108**, 011607 (2016).
[16]Y. Zhu, K. A. Dunn, and A. E. Kaloyeros, J. Mater. Res. **22**, 1292 (2007).
[17]B. H. Choi, Y. H. Lim, J. H. Lee, Y. B. Kim, H. N. Lee, and H. K. Lee, Microelectron. Eng. **87**, 1391 (2010).
[18]J. Gluch, T. Rößler, D. Schmidt, S. B. Menzel, M. Albert, and J. Eckert, Thin Solid Films **518**, 4553 (2010).
[19]M. Ladanov, P. Algarin-Amaris, G. Matthews, M. Ram, S. Thomas, A. Kumar, and J. Wang, Nanotechnology **24** (2013).
[20]J. D. Caldwell *et al.*, Opt. Express **19**, 26056 (2011).
[21]J. C. Ye, Y. H. An, T. W. Heo, M. M. Biener, R. J. Nikolic, M. Tang, H. Jiang, and Y. M. Wang, J. Power Sources **248**, 447 (2014).
[22]H. Sheth, J. Mater. Chem. C **3**, 132 (2015).
[23]T. Dobbelaere, F. Mattelaer, J. Dendooven, P. Vereecken, and C. Detavernier, Chem. Mater. **28**, 3435 (2016).
[24]S. P. Sree, J. Dendooven, J. Jammaer, K. Masschaele, D. Deduytsche, J. D. Haen, C. E. A. Kirschhock, J. A. Martens, and C. Detavernier, Chem. Mater. **24**, 2775 (2012).
[25]J. Dendooven, K. Devloo-Casier, M. Ide, K. Grandfield, M. Kurttepeli, K. F. Ludwig, P. van der Voort, and C. Detavernier, Nanoscale **6**, 14991 (2014).
[26]N. T. Gabriel and J. J. Talghader, Appl. Opt. **49**, 1242 (2010).
[27]M. C. Schwille, J. Barth, T. Schössler, F. Schön, J. W. Bartha, and M. Oettel, Model. Simul. Mater. Sci. Eng. **25**, 1 (2017).
[28]M. Mattinen, J. Hämäläinen, F. Gao, P. Jalkanen, K. Mizohata, J. Räisänen, R. L. Puurunen, M. Ritala, and M. Leskelä, Langmuir **32**, 10559 (2016).
[29]R. L. Puurunen and F. Gao, *2016 14th International Baltic Conference on Atomic Layer Deposition (BALD 2016)*, St. Petersburg, 2–4 October 2016 (IEEE, New York, 2016).
[30]H. C. M. Knoops, E. Langereis, M. C. M. van de Sanden, and W. M. M. Kessels, J. Electrochem. Soc. **157**, G241 (2010).
[31]M. K. Gobbert, V. Prasad, and T. S. Cale, Thin Solid Films **410**, 129 (2002).
[32]G. Prechtl, A. Kersch, G. S. Icking-konert, W. Jacobs, T. Hecht, and H. Boubekeur, *Technical Digest International Electron Devices Meeting*, Washington, DC, 8–10 December 2003 (IEEE, New York, 2003).
[33]J.-Y. Kim, J.-H. Kim, J.-H. Ahn, P.-K. Park, and S.-W. Kang, J. Electrochem. Soc. **154**, H1008 (2007).
[34]R. A. Adomaitis, Chem. Vap. Deposition **17**, 353 (2011).
[35]A. V. Fadeev and K. V. Rudenko, Thin Solid Films **672**, 83 (2018).
[36]A. Yanguas-Gil and J. W. Elam, Chem. Vap. Deposition **18**, 46 (2012).
[37]T. Keuter, N. H. Menzler, G. Mauer, F. Vondahlen, R. Vaßen, and H. P. Buchkremer, J. Vac. Sci. Technol. A **33**, 01A104 (2015).
[38]Y. Miyano, R. Narasaki, T. Ichikawa, A. Fukumoto, F. Aiso, and N. Tamaoki, Jpn. J. Appl. Phys. **57**, 06JB03 (2018).
[39]J. W. Elam, D. Routkevitch, P. P. Mardilovich, and S. M. George, Chem. Mater. **15**, 3507 (2003).
[40]J. Dendooven, D. Deduytsche, J. Musschoot, R. L. Vanmeirhaeghe, and C. Detavernier, J. Electrochem. Soc. **157**, G111 (2010).
[41]J. Musschoot, J. Dendooven, D. Deduytsche, J. Haemers, G. Buyle, and C. Detavernier, Surf. Coatings Technol. **206**, 4511 (2012).
[42]H. Shimizu, K. Sakoda, T. Momose, M. Koshi, and Y. Shimogaki, J. Vac. Sci. Technol. A **30**, 01A144 (2012).
[43]R. I. Masel, *Principle of Adsorption and Reaction on Solid Surfaces* (Wiley, New York, 1996).
[44]R. G. Gordon, D. Hausmann, E. Kim, and J. Shepard, Chem. Vap. Deposition **9**, 73 (2003).
[45]J. Y. Kim, J. H. Ahn, S. W. Kang, and J. H. Kim, J. Appl. Phys. **101**, 073502 (2007).
[46]A. Yanguas-Gil and J. W. Elam, J. Vac. Sci. Technol. A **30**, 01A159 (2012).
[47]M. C. Schwille, T. Schössler, F. Schön, M. Oettel, and J. W. Bartha, J. Vac. Sci. Technol. A **35**, 01B119 (2017).
[48]V. Vandalon and W. M. M. Kessels, J. Vac. Sci. Technol. A **35**, 05C313 (2017).
[49]G. P. Gakis, H. Vergnes, E. Scheid, C. Vahlas, A. G. Boudouvis, and B. Caussat, Chem. Eng. Sci. **195**, 399 (2019).